Journal of Multidisciplinary Engineering Science Studies (JMESS)
ISSN: 2458-925X
Vol. 5 Issue 10, October - 2019

Godunov Type Methods Calculations Of Unsteady Flows Near Blunted Cylinders, Giving Off Opposite Jets

Vladimir I. Pinchukov

In-te of Computational Technologies,
Siberian division of Russian Academy of Sc.,
Novosibirsk, Russia
Email address: pinchvi@ict.nsc.ru,

***Abstract*—Numerical studies of supersonic flows near spherically blunted cylinders, giving off opposite supersonic jets from forehead surfaces, are carried out. Two-dimensional Euler equations of a polytropic gas with the specific heats ratio 1.4 are solved. Self-oscillatory flows are found for the free stream Mach numbers interval [1.1 - 1.7]. Explicit Godunov type first and second orders schemes are used. Comparison of SPL data provided by first order and second orders methods is presented.**

Keywords—Euler equations; CFD studies; self-oscillations; compressible flows;

I. Introduction

This paper is devoted to continuation of a numerical search for unsteady compressible flows, started in [1]. The result of these search is a new family of self-oscillatory flows near blunted cylinders, giving off opposite jets.[2-3]. Implicit third order Runge-Kutta method [4] is used. Next studies of this family are performed here on the base of a first order version of the highly reliable Godunov method [5]. Numerical flow fields, provided by this method, are influenced by the first order scheme dissipation. To evaluate this influence second order two step version of Godunov method is used additionally in present calculations

Flow self-oscillations are supposed here to be resulted from resonance interactions of flow “active” elements, namely, elements, which amplify disturbances. The hypothesis [1] is used that contact discontinuities and intersection points (lines in 3d case) of shocks with shocks or shocks with contact discontinuities compose the flow set of “active” elements. A search for new unsteady flows is conducted by investigations of flows, containing the most number of “active” elements. According to this mechanism of oscillations numerical method for simulations of unsteady flows should provide good correspondence of directions of disturbances propagation for Euler equations and numerical method. Godunove type methods provide good correspondence and may be evaluated as highly proper for application in this CFD field.

Opposite jets, out-flowing from forehead surfaces of blunted bodies, may be used for protecting bodies from heating by a mainstream (see, for example, [6]-[8]). Self-oscillatory regimes are not observed in previous investigations. At the same time calculated here flow fields contain three shock waves, three contact discontinuities and some intersection points [1]. So these flows may be supposed to produce self-oscillations, according to the formulated above hypothesis. It seems that there is contradiction between present results and other investigations. To settle this contradiction it should be noted that, first, flows near blunted bodies with opposite jets are defined by large number of control parameters and depend on body and nozzle forms, consequently, require more thorough investigations, second, subsonic or transonic jets are usually used for cooling of the bodies while present considerations deal with jet Mach numbers M_{jet} ≥2.5.

Supersonic flows near blunted cylinders, giving of

opposite jets [1-3], compose new class of jet self-oscillatory flows. Besides present new family, there are two known jet flows families, containing: 1. Flows near supersonic jets, inflowing to forward facing cavities (see, for example, [9]-[12]); 2. Flows near supersonic jets, impinging on plates [13]-[21].

II. CFD Design Approach

A computational domain and a mesh may be seen in fig. 1. The blunted cylinder wall is shown by a bold line. Opposite supersonic jets outflow from nozzles in forehead parts of blunted cylinders. These jets are supposed to be spherically symmetrical. Jet velocities at exits of nozzles are normal to spherical surfaces.

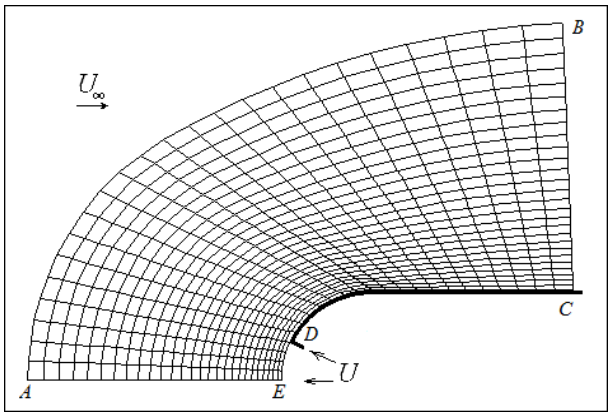

Fig. *1. Mesh and computational domain schematic representation*.

Boundary conditions for computations are zero value of the normal velocity and extrapolation relations for all other variables along the body surface (boundary *DC*), extrapolations on the outflow boundary *BC* at right side of numerical domain (see fig 1), prescribed variables on the inflow forehead boundary AB and on the spherical boundary *DE*, corresponding to the opposite jet, zero value of the radial velocity and extrapolations at symmetry axis *AE.*

Godunov type conservative first order and second order versions of the method [5] with approximate linear solution of Riman problem are employed here. Algorithms of slopes limitation of left and right extrapolation curves in second order two step version of Godunov method are used to damp false oscillations near discontinuities. Review of such algorithms of damping false oscillations are presented in [22]. Navier-Stokes viscous terms are included to Euler equations and the Smagorinsky artificial viscosity [23] is used for additional damping of false oscillations. This viscosity is calculated by equations

$$\mu = \rho |S| (C_s \Delta)^2, \quad |S| = (2 S_{ik} S_{ik})^{1/2},$$

$$S_{ik} = (\partial u_i / \partial x_k + \partial u_k / \partial x_i)/2,$$

$$\Delta = \Delta\xi \Delta\eta (x_\zeta y_\eta - y_\zeta x_\eta)/(\mathrm{Min}(\Delta\xi^2 (x_\zeta^2 + y_\zeta^2), \Delta\eta^2 (x_\eta^2 + y_\eta^2)))^{1/2},$$

where functions $x=x(\xi,\eta)$, $y=y(\xi,\eta)$ perform mapping of the unit square $\{0 \le \xi \le 1, 0 \le \eta \le 1\}$ to a curvilinear quadrangle on the plane of physical variables, $\Delta\xi = 1/N_\zeta$, $\Delta\eta = 1/N_\eta$, N_ζ, N_η - numbers of intervals of the quadrangular mesh in a unit square, C_s - constant, which is chosen in trial computations, $C_s = 0.85$. The 490 × 544 mesh is used usually here.

Numerical calculations deal with dimensionless variables. These variables are defined as relations of initial variables and next parameters of the free stream flow or radiuses of cylinders *r*: p_∞ - for pressure, ρ_∞ - for density, $\sqrt{p_\infty/\rho_\infty}$ - for velocity, *r* – for space variables, $r/\sqrt{p_\infty/\rho_\infty}$ - for time.

The intensity of flow oscillations may be measured by sound pressure level at some point:

$$SPL = 10 \ \mathrm{Log}_{10} (\overline{p'^2} / p_{ref}^2), \quad \overline{p'^2} = \sum_n (p_n - \overline{p})^2 / N,$$

$$p_{ref} = 20\mathrm{mkPa}/p_\infty,$$

where $P_\infty = 101325$Pa (the air pressure under normal conditions) is used since dimensionless variables are dealt here. Sound pressure levels at the intersection point of spherical and cylindrical parts are represented in two tables below.

III. Free stream Mach numbers $1.1 \le M_\infty \le 1.3$.

Studied here flows are defined by five control parameters: M_∞, M_{jet}, ρ_{jet}, p_{jet}, $б_{jet}$ - free stream and jet Mach numbers, jet density, jet pressure, a jet half-angle. Large number of control parameters makes systematic parametric study of these flows too expensive. A search for new self-oscillatory flows is performed by moving step by step in the greater Mach number direction from any initial flows, for example, published in [2], [3]. Results of a search are represented in tables 1-2. Columns 1-2 show free stream and jet Mach numbers, column 3-4 show jet pressure and density, column 5 contains $\sin(б_{jet})$, $б_{jet}$ - a jet half-angle, 6th and 7th columns show results of computations, namely, SPL data at the intersection point of spherical and cylindrical parts of considered bodies. First order Godunov method computational data are represented in the 6th column, second order Godunov method data are represented in the 7th column.

Table1: Sound pressure levels at $1.1 \le M_\infty \le 1.3$.

M_∞	M_{jet}	P_{jet}	P_{jet}	Sin(б)	*SPL*, m. 1	*SPL*, m. 2
1.1	3.0	0.5	0.583	12/30	164.8	166.5
1.1	3.5	0.4	0.625	1/3	172.0	172.3
1.2	4.0	0.292	0.469	1/3	158.6	169.6
1.3	4.5	0.233	0.465	11/30	158.4	170.0
1.3	4.5	0.233	0.465	1/3	162.5	169.8
1.3	4.5	0.233	0.465	9/30	162.2	163.4

Fig. 2 shows the density distribution for the unsteady flow 5 in table 1, first order Godunov method data are pictured. Intensive self-oscillations produce shock waves, moving towards the main bold shock wave, and vortexes, drifting above the cylinder surface.

The pressure history is shown in fig. 3 for this flow. Five points of minimal values of pressure may be seen in this fig. So the main tone period of this flow may be evaluated approximately by the formulae $\tau = (t_5 - t_1)/4 = 3.72$.

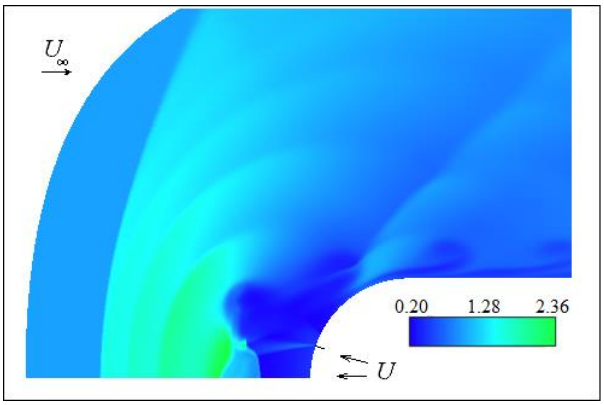

Fig. *2. M_∞ =1.3, the density distribution.*

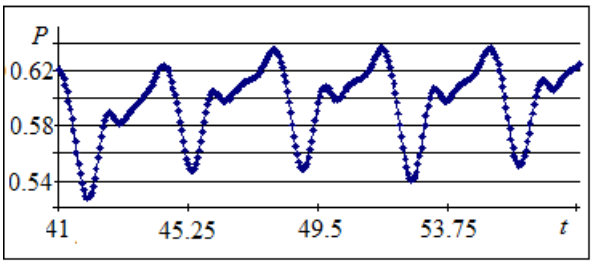

Fig. *3. M_∞ =1.3, the pressure history*.

IV. Free Stream Mach Numbers $1.4 \le M_\infty \le 1.7$.

Results of a CFD search for this Mach numbers interval are represented in table 2.

Table2: Sound pressure levels at $1.4 \le M_\infty \le 1.7$.

M_∞	M_{jet}	P_{jet}	P_{jet}	Sin(б)	*SPL*, m. 1	*SPL*, m. 2
1.4	5.5	0.20	0.434	1/3	169.2	171.8
1.4	5.5	0.25	0.347	1/3	173.6	178.5
1.5	5.5	0.25	0.289	1/3	174.6	175.2
1.5	5.5	0.25	0.347	1/3	164.2	174.4
1.6	5.5	0.25	0.289	1/3	162.3	176.3
1.7	5.5	0.25	0.289	1/3	159.9	175.5
1.7	5.5	0.25	0.347	1/3	164.0	177.0

Fig. 4 shows the density distribution, fig.5 shows the pressure history for the unsteady flow 2 in table 2. First order Godunov method data are pictured in these figs. Intensive self-oscillations produce shock waves, moving towards the main bold shock wave, and vortexes, drifting above the cylinder surface. Six points of minimal values of pressure may be seen in fig. 5. So main tone period of this flow may be evaluated ap-

proximately by the formulae $\tau = (t_6 - t_1)/5 = 4.40$. If to look more attentively at this fig., it may be seen that this flow is periodical with the period $T=2\tau$.

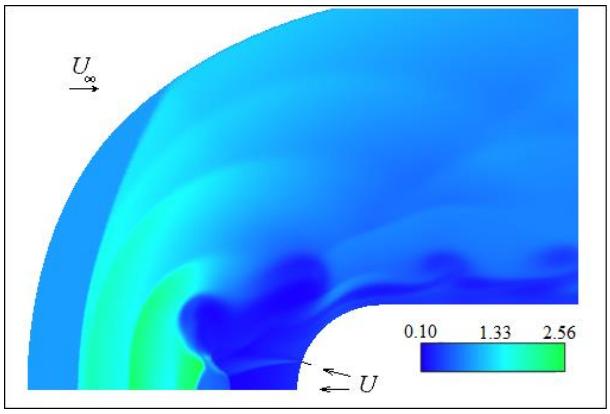

Fig. 4. M_∞ =1.4, the density distribution,

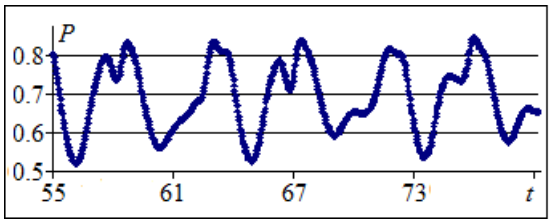

Fig. 5. M_∞ =1.4, the pressure history

Density distributions, considered above, correspond to first order method data. Fig. 6 shows the density distribution for the unsteady flow 7 in table 2, second order Godunov method data are pictured. Intensive self-oscillations produce shock waves, moving towards the main bold shock wave, and vortexes, drifting above the cylinder surface.

Pressure histories are shown in fig. 7 for this flow. First order Godunov method data are painted by dark symbols, second order Godunov method data are painted by rose symbols. At the initial time instant of these histories flow fields correspond to developed self-oscillatory regime in Godunov first order method simulation. Large difference of oscillations intensities and of periods of main modes are seen in fig. 4b. Corresponding difference of SPL data (164db and 177db) may be seen for this variant in the line 7 of table 2. Main modes of these two solutions are defined by periods $\tau = 0.945$ and $\tau = 1.70$. So, significant dissipation of the first order Godunov method damps fast modes and limits intensity of oscillations.

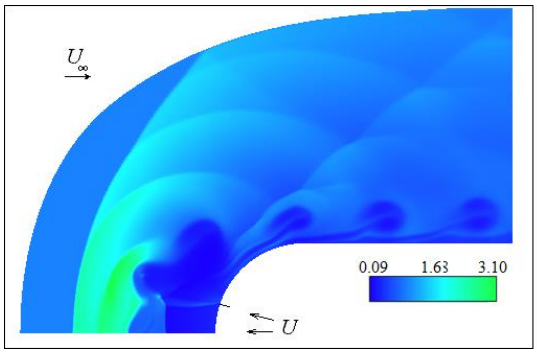

Fig. 6. M_∞ =1.7, the density distribution.

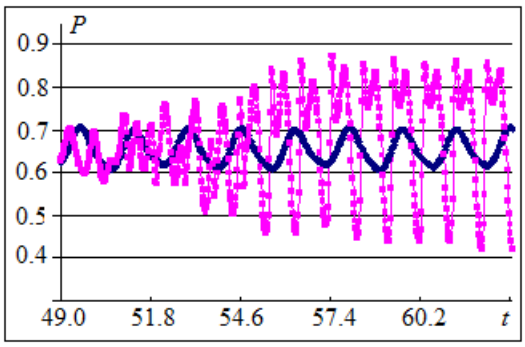

Fig. 7. M_∞ =1.7, pressure histories, first and second order methods.

Similar large difference of oscillation intensities, calculated for first and second order methods data, may be seen in lines 3-6 in tables 1 and 2, 4-7 in table 2. Some lines contain variants with closed first and second orders SPL data (vars. 1, 2 in table1 and vars. 1, 3 in table 2). It is interesting to note that in all cases main tones of considered first and second orders methods solutions are different, namely, main tone periods are significantly longer in the case of the first order method then in the case of the second order method. There are significant number of variants, omitted in tables 1-2, which are self-oscillatory in second orders Godunov method simulations, but are steady or contain only negligible oscillations in the case of first orders Godunov method simulations.

To investigate more carefully influence of the first order dissipation on a numerical solution this flow (line 7 in table2) is calculated additionally on the 971 × 999 grid. Numerical solution is interpolated from the 490 × 544 grid to the 971 × 999 grid at initial time instant t=49.0 (see fig. 4b). Fig. 5 shows density histories, 490 × 544 data are drawn by dark symbols, 971 × 999 data are drawn by rose symbols. Intensity of self-oscillations increased and short period modes appeared to final time instant in the case of the 971 × 999 mesh. This solution seems to be more like the second order solution at the 490 × 544 grid. It is interesting to note, that the second order solution requires computer work about four times less then computer work of first order method for the 971 × 999 mesh.

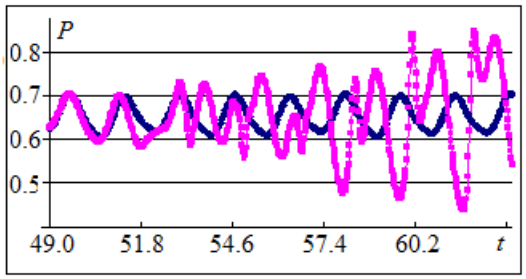

Fig. 8. *M_∞ =1.7, pressure histories, 490× 544 and 971× 999 grids.*

Significant changeability of computational data is demonstrated by considered above results. It is a feature of this family of unsteady flows, which may be explained by high role of contact discontinuities in "active" elements interactions. It should be noted that present flows contains three contact discontinuities, namely, long contact discontinuity, separating the free flow and the jet flow, contact discontinuity, corresponding to the boundary of opposite jet, and contact discontinuity, corresponding to the boundary of the separation zone near the jet and the body wall. Kelvin-Helmholtz instability of these contact discontinuities produces disturbances and their interactions may be supposed to take important role in generation of self- oscillations. Particularly, the first contact discontinuity is seen to be disturbed as a result of instability by waves, which are drifted along the cylinder surface (see, for example, fig 6).

Growth of disturbances, resulted from instability, highly depends on the dissipation of a numerical method. This dependence leads to changeability of numerical results, mentioned above. The question is which flow may be observed experimentally. It seems, that laminar flows may by close to second order method solutions, highly turbulent flows are influenced by turbulent dissipation and oscillations may be partly or fully damped similarly to damping in present numerical first order method simulations. Of course, this question require additional investigations.

Consideration of presented here and omitted variants shows, that flows are steady for sufficiently large jet half-angles, jets are destroying and a process of this destroying produces self-oscillations for middle jet half-angles, jets get large distance from spherical blunts of cylinders (this flows are not shown here) for sufficiently small jet half-angles. As a jet velocity or jet pressure or jet density decreases, a jet gets less distance from spherical blunt as a result of jet braking by a contrary free stream. A steady state regime takes place, if this distance is sufficiently small.

V. Conclusions

Interactions of supersonic streams with blunted bodies, giving off supersonic jets, are studied. Previous investigations [2]-[3] allowed to find unsteady regimes of these interactions at free stream Mach numbers, closed to 1. The Mach numbers interval $1.1 \le M_\infty \le 1.7$ of unsteady regimes is established here.

Significant changeability of computational results is a feature of this family of unsteady flows due to strong influence of the numerical method dissipation on disturbances generation resulted from a Kelvin-Helmholtz instability of three contact discontinuities available in these flows. It may be supposed, that laminar flows may be close to second order method solutions, highly turbulent flows are influenced by turbulent dissipation and oscillations may be partly or fully damped similarly to damping in present numerical first order method simulations, but this question require next investigations.

To define more exactly regions with any flow regimes in 5D space of control parameters, both CFD modeling and experimental studies are necessary.

References:

[1] V.I. Pinchukov, "Modeling of self-oscillations and a search for new self-oscillatory flows," Mathematical Models and Computer Simulations, 4(2), 2012, pp. 170–178.

[2] V.I. Pinchukov, "Numerical simulations of self-oscillatory flows near blunted bodies, giving off opposite jets," Intern. J. of Mechanical Engineering and Applications 2(1), 2014, pp. 5-10.

[3] V.I. Pinchukov, "Self-oscillatory flow near blunted bodies, giving off opposite jets: CFD Study," Intern. J. of Engineering and Innovative Technology, 6(5), 2016, pp. 41-46.

[4] V.I. Pinchukov, "Numerical solution of the equations of viscous gas by an implicit third order Runge–Kutta scheme," Comput. Mathem. And Mathem. Physics, Vol. 42(6), 2002, pp. 898-907.

[5] S.K. Godunov, "A difference method for numerical calculation of discontinuous solutions of the equations of hydrodynamics," Mat. Sb. *(N.S.)*, 47(89):3, 1959, pp. 271–306.

[6] C.H.E. Warren, "An experimental investigation of the effect of ejecting a coolant gas at the nose of a bluff Body," J. of Fluid Mechanics, Vol.8, No. 3, 1960, pp. 400-417.

[7] K. Hayashi, S. Aso**,** "Effect of pressure ratio on aerodynamic heating reduction due to opposing jet," AIAA 2003-4041, 2003.

[8] I. Tamada, S. Aso, Y. Tani**,** "Reducing aerodynamic heating by the opposing jet in supersonic and hypersonic flows," AIAA 2010-991, 2010.

[9] J. Hartmann, "On a new method for the generation of sound waves," Phys. Rev., 20(6), 1922, pp. 719-726.

[10] S. Murugappan, E. Gutmark, "Parametric study the Hartmann–Sprenger tube," Experiments in Fluids, 38(6), 2005, pp. 813-823.

[11] J. Kastner, M. Samimy, "Develoment and characterization of Hartmann tube fluid actuators for high-speed control," American Instiute of Aeronautics and Astronautics J., 40(10), 2002, pp. 1926–1934.

[12] G. Raman, E. Envia, T.J. Bencic, "Jet cavity interaction tones," American Institute of Aeronautics and Astronautics J., 40(8), 2002, pp. 1503–1511.

[13] W. Wu, U. Piomelli, "Large-eddy simulation of impinging jets with embedded azimuthal vortices," J. of Turbulence, 16(10), 2014, pp. 44- 66.

[14] C.-Y. Kuo, A. P. Dowling, "Oscillations of a moderately underexpanded choked jet impinging upon a flat plate," J. Fluid Mech., 315, 1996, pp. 267–291.

[15] Y. Sakakibara, J. Iwamoto, "Numerical study of oscillation mechanism in underexpanded jet impinging on plate," J. Fluids Eng., 120, 1998, pp. 477-481.

[16] B. Henderson, J. Bridges, M. Wernet, "An experimental study of the oscillatory flow structure of tone-producing supersonic impinging jets," J. Fluid Mech., 542, 2005, pp. 115–137.

[17] J. Berland, C. Bogey, C. Bailly, "Numerical study of screech generation in a planar supersonic jet," Phys. Fluids, 19, 2007, pp. 75-105.

[18] D.J. Bodony, S.K. Lele, "On using large-eddy simulation for the prediction of noise from cold and heated turbulent jets," Phys. Fluids, 17, 2005.

[19] C. Bogey, C. Bailly, "Computation of a high Reynolds number jet and its radiated noise using large eddy simulation based on explicit filte- ring," Comput. Fluids, 35, 2006, pp. 1344-1358.

[20] T. Cheng, K. Lee, "Numerical simulations of underexpanded supersonic jet and free shear layer using WENO schemes," Int. J. Heat Fluid Flow, 26(5), 2005, pp. 755–770.

[21] V.I. Pinchukov, "Numerical modeling of unsteady flows with transient regimes," Comput. Mathem. and Mathem. Physics, 49 (10), 2009, pp. 1844– 1852.

[22] P. Woodward, "The numerical simulation of two-dimensional fluid flow with strong shocks," J. of Comput. Physics, 54, 1984, pp. 115-173.

[23] J. Smagorinsky, "General circulation experiments with the primitive equations. I. The basic experiment," Monthly Weather Review, 91, 1963, pp. 99-164.